NEUROSCIENCE

A lateral hypothalamus to basal forebrain neurocircuit promotes feeding by suppressing responses to anxiogenic environmental cues

Ryan M. Cassidy[1,2,3], Yungang Lu[1], Madhavi Jere[4], Jin-Bin Tian[1,5], Yuanzhong Xu[1], Leandra R. Mangieri[1,3], Blessing Felix-Okoroji[6], Jennifer Selever[7,8,9], Yong Xu[10], Benjamin R. Arenkiel[7,8,9], Qingchun Tong[1,3,11]*

Animals must consider competing information before deciding to eat: internal signals indicating the desirability of food and external signals indicating the risk involved in eating within a particular environment. The behaviors driven by the former are manifestations of hunger, and the latter, anxiety. The connection between pathologic anxiety and reduced eating in conditions like typical depression and anorexia is well known. Conversely, anti-anxiety drugs such as benzodiazepines increase appetite. Here, we show that GABAergic neurons in the diagonal band of Broca (DBB^{GABA}) are responsive to indications of risk and receive monosynaptic inhibitory input from lateral hypothalamus GABAergic neurons (LH^{GABA}). Activation of this circuit reduces anxiety and causes indiscriminate feeding. We also found that diazepam rapidly reduces DBB^{GABA} activity while inducing indiscriminate feeding. Our study reveals that the LH^{GABA}→DBB^{GABA} neurocircuit overrides anxiogenic environmental cues to allow feeding and that this pathway may underlie the link between eating and anxiety-related disorders.

INTRODUCTION

Animals must constantly determine whether it is safe to eat and overcome environmentally driven anxiety to allow feeding. In a risky or uncertain environment, animals display anxiety with heightened food selectivity (*1*–*3*). This may explain the tight connection between picky eating and anxiety associated with heightened sensory sensitivity in humans (*4*, *5*). Further, maladaptive responses to sensory signals, especially related to food, underpin the connection between eating and anxiety commonly seen in diseases such as autism and anorexia nervosa (*6*, *7*). However, brain regions mediating the connection between anxiety and hunger, especially those related to behavioral inhibition in the face of a risky environment, are not yet known. The basal forebrain is known for its role in processing sensory information, mediating arousal, and governing behavioral inhibition (*8*–*10*). Clinically, dementia types with early involvement of the basal forebrain have increased appetite and altered eating habits (*11*, *12*). Our recent work has shown that ablation of cholinergic neurons, a subset of GABA(γ-aminobutyric acid receptor type A)ergic neurons, in the diagonal band of Broca (DBB) within the basal forebrain increases feeding and results in obesity (*13*). Thus, the DBB is likely to be involved in the connection between anxiety and feeding.

Hypothalamic neurons also regulate feeding and associated emotional states. Agouti-related peptide neurons, for example, promote feeding with changes in valence, anxiety, and aggression during negative energy balance (*14*–*18*). GABAergic neurons of the lateral hypothalamus (LH^{GABA}) also alter the behavioral phenotype in response to hedonic stimuli (*19*). Selective activation of a subset of their projections promotes positive reinforcement, predatory attack, and feeding behavior (*20*–*24*). How hypothalamic regulation of feeding interfaces with anxiogenic environmental cues remains unknown. Here, we sought to test the possibility that a heretofore undescribed neurocircuit between the LH and DBB mediates some of these effects.

RESULTS

LH^{GABA} neurons project to and inhibit DBB neurons to drive feeding

To demonstrate an LH-specific projection to the DBB, we used pancreatic and duodenal homeobox 1 (*Pdx1*)–*Cre* mice. Previous research in our laboratory has demonstrated that injecting cre-dependent viruses to the LH region results in selective expression within LH (LH^{Pdx1}) neurons and not the surrounding area (*22*, *23*). LH^{Pdx1} neurons targeted with AAV-Flex-ChR2-EYFP showed prominent projections to the DBB (fig. S1). To selectively activate these projections, we implanted an optic fiber over the DBB (Fig. 1A). Photostimulation induced feeding in $LH^{Pdx1\text{-}ChR2}$ mice but had no effect on $LH^{Pdx1\text{-}GFP}$ controls (fig. S2A). Since LH^{Pdx1} neurons are a mix of GABAergic and glutamatergic neurons, we used brain slice electrophysiology of postsynaptic DBB neurons to determine the postsynaptic current elicited after optogenetic stimulation of $LH^{Pdx1\text{-}ChR2}$ terminals in that area. Since only inhibitory postsynaptic currents (oIPSCs) were observed, we concluded that these projections were primarily GABAergic (fig. S2, B and C).

[1]Brown Foundation Institute of Molecular Medicine for the Prevention of Human Diseases, UTHealth McGovern Medical School, 7000 Fannin St., Houston, TX 77030, USA. [2]MSTP, The University of Texas McGovern Medical School and MD Anderson Cancer Center UTHealth Graduate School of Biomedical Sciences, 6767 Bertner Avenue S3.8344 Mitchell BSRB, Houston, TX 77030, USA. [3]Neuroscience Program, The University of Texas MD Anderson Cancer Center UTHealth Graduate School of Biomedical Sciences, 6767 Bertner Avenue S3.8344 Mitchell BSRB, Houston, TX 77030, USA. [4]Vassar College, 124 Raymond Avenue, Poughkeepsie, NY 12604, USA. [5]Department of Integrative Biology and Pharmacology, UTHealth McGovern Medical School, 6431 Fannin St., Houston, TX 77030-1892, USA. [6]Rice University, 6100 Main St., Houston, TX 77005-1892, USA. [7]Intellectual and Developmental Disabilities Research Center, Neuroconnectivity Core, Baylor College of Medicine, One Baylor Plaza, Houston, TX 77030, USA. [8]Department of Neuroscience, Baylor College of Medicine, One Baylor Plaza, S640, Houston, TX 77030, USA. [9]Jan and Dan Duncan Neurological Research Institute, Texas Children's Hospital, 6621 Fannin St., Houston, TX 77030, USA. [10]Children's Nutrition Research Center, Department of Pediatrics, Baylor College of Medicine, 1100 Bates St., Houston, TX 77030, USA. [11]Department of Neurobiology and Anatomy, UTHealth McGovern Medical School, 6431 Fannin St., Suite MSB 7.046 Houston, TX 77030, USA.
*Corresponding author. Email: qingchun.tong@uth.tmc.edu

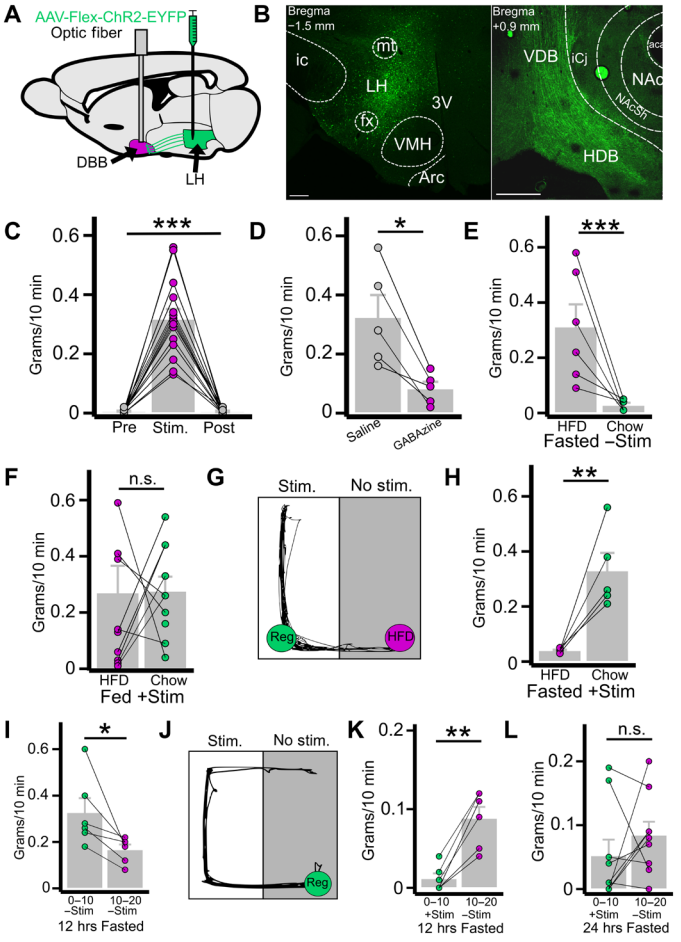

Fig. 1. Activation of LH^{GABA}→DBB projections drives indiscriminate feeding. (**A**) Diagram demonstrating LH injection with AAV-Flex-ChR2-EYFP and implantation of optic fiber over the DBB. (**B**) Representative coronal slices of LH$^{Vgat\text{-}ChR2\text{-}EYFP}$ (left) and EYFP+ fibers in the DBB (right). Scale bars, 250 μm. VMH, ventromedial hypothalamic nucleus; VDB, vertical limb of the DBB; HDB, horizontal limb of the DBB. (**C**) Food intake of fed mice during 10-min periods before (pre), during (stim), and after (post) photostimulation of LH^{GABA}→DBB projections (n = 15, P < 0.001). (**D**) Effect of DBB pretreatment with GABAzine [γ-aminobutyric acid type A (GABA-A) receptor antagonist] or saline on photostimulation-induced feeding (n = 5, P = 0.015). (**E** and **F**) Mouse preference for high-fat diet (HFD) or chow in the fasted state (E; n = 6, P = 0.019) and in the fed state with photostimulation (F; n = 9, P = 0.96). (**G**) Representative trace of a single mouse's movement during competitive choice test. Regular chow (reg) is paired with photostimulation. (**H**) photostimulation-paired chow consumption compared to nonpaired HFD consumption (n = 5, P = 0.011). (**I**) Food consumption in 10-min increments upon food exposure after 12-hour fasting (n = 6, P = 0.028). (**J**) Representative trace of mouse movement when choosing between photostimulation or chow consumption after 12 hours (hrs) of fasting. (**K** and **L**) Food consumption when choosing between chow and photostimulation after 12 hours during the photostimulation period (0 to 10 min) and after photostimulation is ended (10 to 20 min) (K; n = 6, P = 0.001) and 24-hour fasting (L; n = 9, P = 0.34). n.s., not significant. *P < 0.05; **P < 0.01; ***P < 0.001.

We also used two trans-synaptic tracing strategies to further confirm the existence and molecular identity of the LH→DBB projection. The first strategy used a single-synapse anterograde virus, AAV1, carrying a plasmid encoding Cre (*25*). Injection into the LH of Ai9+ animals revealed cre activity in the DBB (fig. S3, A to C); antibody staining against choline acetyltransferase revealed that most of downstream neurons were cholinergic (fig. S3, D to I). The second strategy used a retrogradely transported virus, rAAV2-retro, carrying a plasmid encoding Cre and H2B::Venus (*26*). Injection into the DBB revealed selective expression within the DBB and upstream expression within the LH (fig. S4, A to C); antibody staining revealed that these neurons were not substantially colocalized with a melanin-concentrating hormone (fig. S4, D to F). We did identify a subset of presynaptic neurons in the LH that colocalized with orexin A (the image with greatest colocalization is presented in fig. S4, G to I). Previous research has demonstrated a role for orexin in the basal forebrain in the sleep/wake cycle (*27*). Nonetheless, our data on feeding and predominant IPSCs recorded from photostimulating LH^{Pdx1}-Cre neuron projections suggest a potential dominance of GABAergic projections in the LH→DBB pathway.

Thus, we used *Vgat-cre* mice (*28*) to selectively target LH^{GABA} neurons (LH^{Vgat} or LH^{GABA}) for optogenetic manipulations. Targeting LH^{Vgat} neurons with AAV-Flex-ChR2 (LH$^{Vgat\text{-}ChR2}$) revealed dense fibers in the DBB (Fig. 1B). Similarly, labeling LH^{Vgat} neurons with AAV-Flex-Synaptophysin::EGFP revealed specific GABAergic synaptic terminals in the DBB (fig. S5). These observations are in accordance with our data showing only some overlap between DBB-projecting neurons and orexin+ (and none with MCH+) neurons in the LH, as these have been demonstrated to be Vgat negative (*29*, *30*).

Activation of LH$^{Vgat\text{-}ChR2}$→DBB projections induced rapid, light-locked feeding behavior, recapitulating our findings with LH$^{Pdx1\text{-}cre}$ mice (Fig. 1C and movie S1). LH$^{Vgat\text{-}ChR2}$ light-induced feeding was prevented by pre-microinjection of GABAzine, a GABA$_A$ receptor antagonist, to the DBB (Fig. 1D). From these data, we conclude that the LH^{GABA}→DBB neurocircuit promotes feeding. Further, the local injection of GABAzine demonstrates that the feeding effect that we observed is not due to backpropagation of action potentials to LH^{Vgat} somata or axon collaterals.

LH^{GABA}→DBB activation alters preference for palatable foods

Since feeding behavior is influenced by food palatability, we next explored whether the observed feeding was dependent on the evaluated palatability of the food to be consumed. This is particularly interesting given that activation of somatostatin-positive neurons (likely also GABAergic) in the basal forebrain selectively induced consumption of a palatable food for rodents, high-fat diet (HFD) (*31*). As expected, control mice in the fasted (12 hours) state selectively consumed HFD and not standard chow (Fig. 1E). However, LH^{GABA}→DBB activation in the fed state elicited indiscriminate consumption of both chow and HFD (Fig. 1F). This indicates an alteration in the evaluation of the palatability of the food. To test the extent of altered food palatability caused by circuit activation, we next created a competition paradigm, where fasted mice must choose between chow paired with photostimulation and unpaired HFD; they uniformly preferred stimulation-paired chow (Fig. 1, G and H). Last, to test whether circuit activation is merely magnifying hunger or having other effects with positive valence, we extended the competition paradigm to force mice to choose either photostimulation or chow consumption over 10 min. The pairing was then removed, and food consumption over the next 10 min was measured to determine whether mice retained hunger after ceasing stimulation. As expected, in the control condition, mice approached food right away and ate food during both 10-min

epochs (Fig. 1I). However, when forced to choose between photostimulation and food, mice refrained from eating until stimulation was removed (Fig. 1, J and K). Prolonged fasting (24 hours) reduced this preference (Fig. 1L), suggesting that activation is not sufficient to overcome intense physiologic hunger induced by 24-hour fasting.

LH^{GABA}→DBB activation reduces anxiety

Given the results of the competition experiments, we next examined how circuit activation affects behavior in the absence of food altogether. First, we established that activation has a positive valence using the real-time place preference (RTPP) test. In the RTPP test, mice are allowed to move freely between sides of the chamber, with one side paired with photostimulation. $LH^{Vgat\text{-}ChR2}$ mice preferred the area coupled to photostimulation, whereas $LH^{Vgat\text{-}GFP}$ had no preference (Fig. 2, A and B). Notably, there was no difference in locomotion within the paired area (Fig. 2C). We next tested mouse behavior on the open-field test (OFT), where the entire chamber is paired with photostimulation; in this case, mice spent more time in the center and moved more in the OFT (Fig. 2, D to F). The observed increase in movement may reflect food seeking, since food availability reduced locomotion (fig. S6). This may also explain why the example movement trace in the absence (Fig. 2A, bottom) of food covers greater area than in the presence (Fig. 1, G and J) of food.

To test the extent of positive valence encoded by photostimulation, we tested whether mice were willing to overcome the inherent anxiety of being in the center to receive photostimulation. They demonstrated preference for the center when it was paired with stimulation (Fig. 2G). However, this preference was quickly lost once photostimulation was removed, even after 7 days of training on the conditioned place preference (CPP) test. (Fig. 2H). These results suggest that the positive valence effect of circuit activation may be primarily related to its alleviation of anxiety, rather than independently rewarding.

Circuit-mediated reduction in anxiety allows for food consumption

Given the two major behavioral phenotypes observed—reduction in anxiety and increase in hunger—we next sought to examine the causal relationship between these two behaviors. First, we examined whether stimulation results in a greater amount of food consumed per minute or a faster food approach (i.e., reduced latency to onset of feeding). Notably, shorter latency to food consumption is a classic marker of reduced anxiety and is a standard metric used to judge the efficacy of anti-anxiety medication (*32*). We found that photostimulation of fed mice reduced latency to onset of feeding as compared to mice that fasted for 24 hours (Fig. 2I). However, it does not seem to indicate a substantial increase in hunger, as the total amount of food consumed was comparable and there was no difference in the feeding rate from onset of consumption to end of test (Fig. 2, J and K).

To further examine the interaction between anxiety and hunger, we explored how placement of HFD on the open or closed arm of an elevated plus maze (EPM) with regular chow on the converse arm affected consumption after fasting (fig. S7, A and B). It is well established that being on the open arm is aversive to rodents and that they strongly prefer the closed arm. Our earlier data (Fig. 1E) indicate that mice naturally prefer HFD over chow when given equal access. Coincident with this, when HFD is located on the closed arm, fasted mice began eating HFD immediately and never touched the chow. However, in the flipped condition, there were increased latency to HFD approach, reduced HFD consumption, decreased latency to chow approach, and increased chow consumption (fig. S7, C to F).

Given that placing palatable food on the open arm reduced its value, we next isolated the effect of food placement on feeding behavior (Fig. 2L). Fasted mice showed reduced latency and increased consumption when food was placed on the closed arm as opposed to the open arm (Fig. 2, M and N). Last, activation of the LH^{GABA}→DBB neurocircuit markedly reduced the latency to feeding on the open arm while producing a comparable amount of food consumption (Fig. 2, O and P). From these results, we concluded that (i) anxiety imposed by environment substantially affects both feeding behavior and food choice and (ii) LH^{GABA}→DBB activation reduces this environmental anxiety to allow feeding to occur.

LH^{GABA} neurons specifically target DBB^{GABA} neurons

Having established the behavioral consequences of circuit activation, we next explored what types of neurons within the DBB are postsynaptic to LH^{GABA}→DBB projections. The DBB contains both glutamatergic and GABAergic neurons; the latter includes acetylcholine and somatostatin co-releasing neurons (*31*, *33*, *34*). First, we used a double-injection method of ChR2 into the LH and a cre-dependent fluorescent label in the DBB of *Vgat*-cre or *Vglut2*-cre mice and then performed brain slice electrophysiology (Fig. 3A). In *Vgat*-cre, we targeted the LH with AAV-Flex-ChR2-EYFP and the DBB with AAV-DIO-hM3Dq-mCherry (marking LH^{Vgat} fibers with EYFP and DBB^{Vgat} neurons with mCherry). In *Vglut2-cre*, we targeted the LH with AAV-Fas-ChR2-mCherry and the DBB with AAV-Flex-EGFP. The Fas-ChR2 vector is "Cre-Off," such that only neurons that do not express Cre will express ChR2 (*35*). This means that $LH^{Non\text{-}Vglut2}$ fibers will be marked with mCherry and that DBB^{Vglut2} somata will be marked with enhanced green fluorescent protein (EGFP). Patching the fluorescent cell bodies in the DBB allowed molecular identification of the downstream target. From all neurons recorded, only DBB^{GABA} neurons were shown to receive inhibitory input (Fig. 3, B and C).

We next sought to validate these data in vivo using a similar targeting strategy (Fig. 3A). *Vgat-cre* mice received an injection of AAV-Flex-ChR2 into the LH, and AAV-Flex-DIO-hM3Dq-mCherry [a synthetic excitatory receptor that can be activated with clozapine-*N*-oxide (CNO); see fig. S8, top, for fluorescent pattern and CNO-induced c-fos expression]. Pretreatment of $LH^{Vgat\text{-}ChR2}$:$DBB^{Vgat\text{-}hM3Dq}$ mice with CNO substantially reduced the amount of photostimulation-induced feeding (Fig. 3D). We also used the converse strategy, where *Vglut2-cre* mice received an injection of AAV-Fas-ChR2 in the LH and AAV-Flex-hM3Dq-mCherry in the DBB (fig. S8, bottom). Pretreatment of $LH^{Vglut2:Fas\text{-}ChR2}$:$DBB^{Vglut2\text{-}hM3Dq}$ mice with CNO had no effect on stimulation-induced feeding (Fig. 3E).

To further confirm the LH^{GABA}→DBB^{GABA} connection, we used a real-time fiber photometry of calcium-dependent fluorescence from LH^{GABA} and DBB^{GABA} neurons expressing AAV-DIO-GCaMP6m (*36*). After fasting, simultaneous recording of $LH^{Vgat\text{-}GCaMP6m}$ and $DBB^{Vgat\text{-}GCaMP6m}$ neurons showed that, as LH^{GABA} neurons increased their activity (Fig. 3F, top), DBB^{Vgat} neurons showed a concomitant decrease (Fig. 3F, bottom) specifically during the feeding bout.

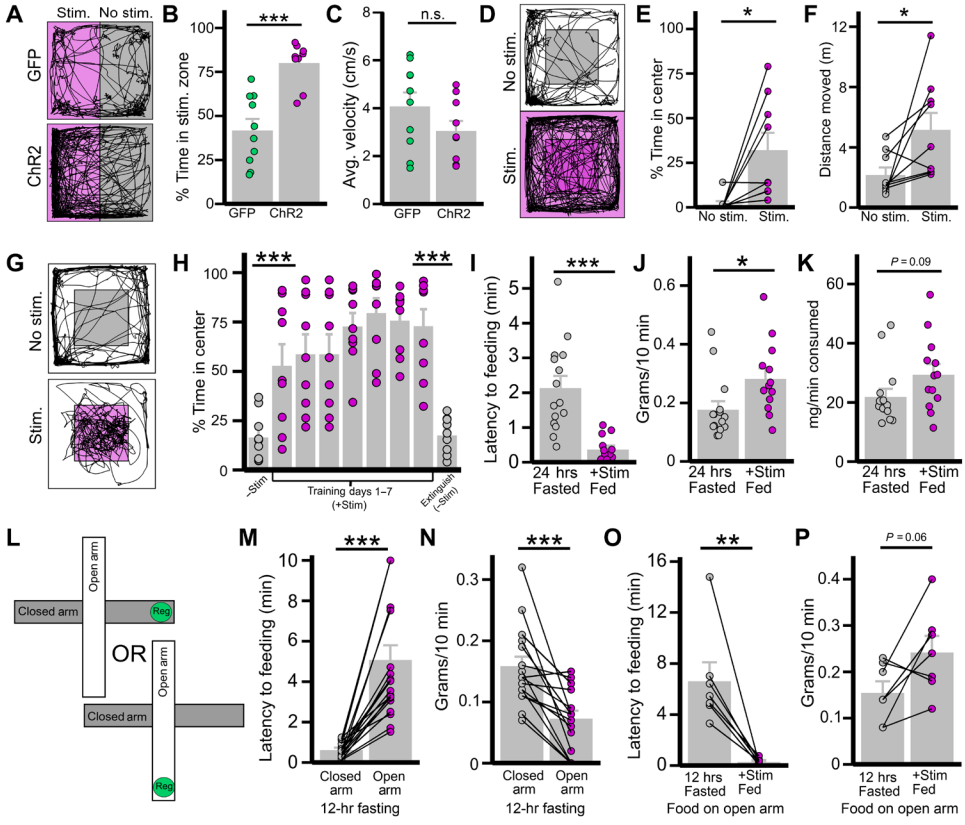

Fig. 2. Activation of LH^{GABA}→DBB projections reduces anxiety. (**A** to **C**) Effect of photostimulation of LH^{GABA}→DBB projections on RTPP test (n = 14 per group). (A) Representative trace of mouse movement (black) in gray zone and photostimulation-paired magenta zone (stim zone). (B and C) Comparison between LH$^{Vgat\text{-}ChR2}$ mice and LH$^{Vgat\text{-}GFP}$ mice on percentage of testing time spent in stim zone (B; $P < 0.001$) and average velocity in stim zone (C; $P = 0.15$). GFP, green fluorescent protein. (**D** to **F**) Ten-minute OFT in LH$^{Vgat\text{-}ChR2}$ mice (n = 9): Photostimulation effect on mouse movement (black trace) on OFT (D; center is shaded gray) and effect of photostimulation on percentage of time in center (E; $P = 0.015$) and distance traversed (F; $P = 0.038$). (**G** and **H**) CPP test for photostimulation-paired center in LH$^{Vgat\text{-}ChR2}$ mice over 20 min per test (n = 9): mouse movement in chamber with (magenta) or without (gray) photostimulation-paired center (G), and effects of training on percentage of time spent in center initially without stimulation compared to the first training day ($P = 0.007$) and last training day to no-photostimulation extinction phase (24 hours after day 7; $P < 0.001$) (H). (**I** to **K**) Effect of photostimulation of LH^{GABA}→DBB projections on feeding behaviors compared to 24-hour fasted mice (n = 15 per group): Effect of photostimulation on latency to feeding (I; $P < 0.001$) and food consumed (J; $P = 0.022$). (K) Food consumed per minute of feeding ($P = 0.09$). (**L** to **N**) Influence of food location on open or closed arm of EPM on fasted-refeeding response in control mice (n = 20). (L) Schematic showing two testing conditions: food placed on the closed (gray) arm or food placed on the open (white) arm. (M) Latency to the first bite of food in closed or open condition ($P < 0.001$). (N) Consumption 10 min following first bite ($P < 0.001$). (**O** and **P**) Influence of activation of LH^{GABA}→DBB on feeding when food was on open arm of EPM (n = 7). (O) Latency to the first bite of food on open arm when fasted or fed and with (+stim) laser stimulation ($P = 0.004$). (P) Consumption 10 min following the first bite ($P = 0.06$). *$P < 0.05$; **$P < 0.01$; ***$P < 0.001$.

Last, we sought to demonstrate in vivo that activation of LH$^{Vgat\text{-}ChR2}$ neurons produces a time-locked reduction in activity of DBB^{Vgat} neurons. Simultaneous photostimulation of LH$^{Vgat\text{-}ChR2}$ cell bodies and fiber photometry recording from DBB$^{Vgat\text{-}GCaMP6m}$ cell bodies demonstrated both a pulse frequency–dependent and a pulse duration–dependent reduction in DBB fluorescence (Fig. 3, G and H). Together, these results convinced us that LH^{GABA} neurons specifically inhibit DBB^{GABA} neurons in real time, with the strength of LH^{GABA} activation producing greater amounts of DBB^{GABA} inhibition.

DBB^{GABA} neurons are highly sensitive to anxiogenic environmental cues

Having demonstrated the specific connection between LH^{GABA} and DBB^{GABA} neurons, we then sought to look at the conditions in which DBB^{GABA} neurons are activated. We monitored activities of DBB$^{Vgat\text{-}GCaMp6m}$ neurons (Fig. 4, A and B) in several conditions. We observed that voluntary interaction with a novel object correlated with increased DBB$^{Vgat\text{-}GCaMP6m}$ activity during the period of active investigation of the novel object; this was repeatable across interactions and between mice (Fig. 4C, picture inset demonstrating what was coded as stimulus onset, and movie S2). In addition, both looming threat (Fig. 4D) and loud sound (Fig. 4E) stimuli increased DBB$^{Vgat\text{-}GCaMP6m}$ activity. Each of these is a sign of danger for a laboratory mouse (*1*, *37*, *38*) and indicates that these neurons are involved with heightened attention to anxiogenic stimuli. We also found the converse effect, where DBB$^{Vgat\text{-}GCaMP6m}$ neurons showed decreased activity during feeding bouts, consistent across feeding bouts and between mice (Fig. 4, F and G, and movie S3). Last, treatment with diazepam, an anti-anxiety benzodiazepine known to reduce latency to food consumption (*32*), reduced DBB$^{Vgat\text{-}GCaMP6m}$ activity (Fig. 4, H and I). We found that administering diazepam to fed mice caused feeding (Fig. 4J). Further, administration to

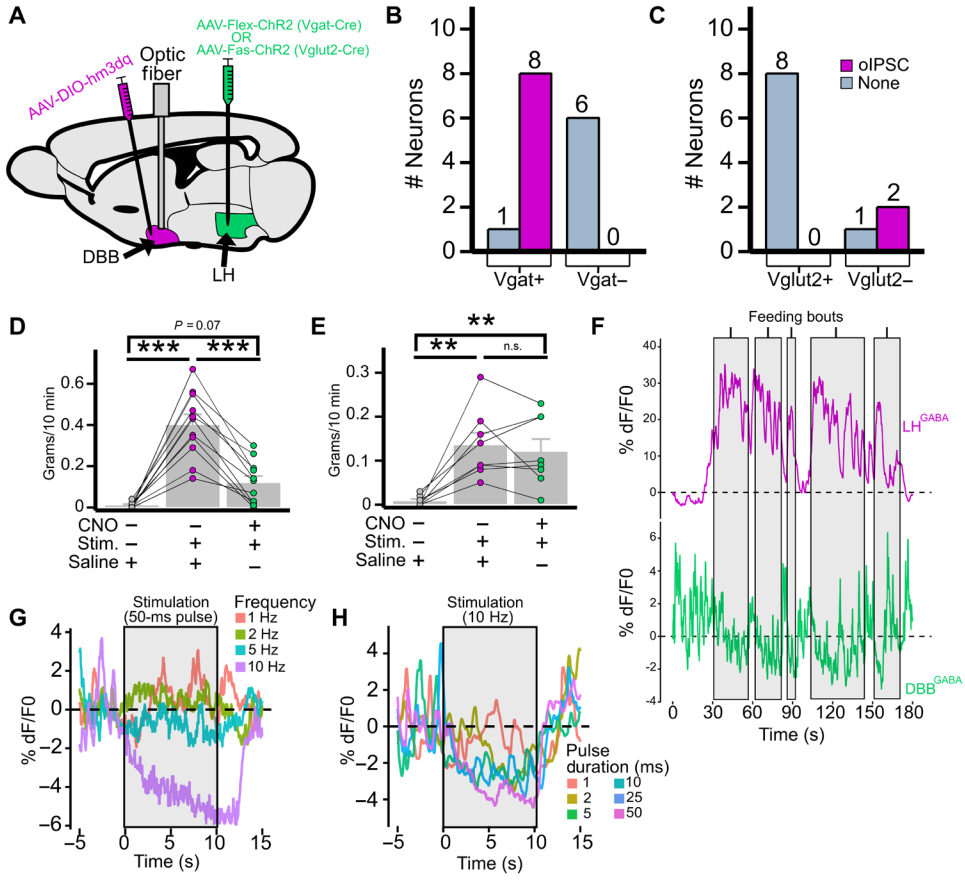

Fig. 3. DBB^{GABA} neurons mediate the effect of LH^{GABA}→DBB projections. (**A** to **C**) DBB^{GABA} neurons receive direct synaptic input from LH^{GABA} neurons. (A) Schematic showing *Vgat-cre* mice receiving LH injection of AAV-Flex-ChR2 (LH$^{Vgat\text{-}ChR2}$) and DBB injection of AAV-DIO-hM3Dq-mCherry and implant of optic fiber (DBB$^{Vgat\text{-}hM3Dq}$), and *Vglut2-cre* mice receiving LH$^{Vglut2\text{-}Fas\text{-}ChR2}$:DBB$^{hM3Dq:fiber}$. (B and C) Brain slice electrophysiology of oIPSC in DBB$^{mCherry+}$ and DBB$^{mCherry-}$ neurons of LH$^{Vgat\text{-}ChR2}$:DBB$^{Vgat\text{-}hM3Dq\text{-}mCherry}$ mice (B; $n = 3$) and LH$^{Vglut2\text{-}Fas\text{-}ChR2}$:DBB$^{Vglut2\text{-}hM3Dq\text{-}mCherry}$ mice (C; $n = 2$). (**D** and **E**) Effect of CNO-mediated activation of DBB^{hM3Dq} on photostimulation-induced feeding in LH$^{Vgat\text{-}ChR2}$:DBB$^{Vgat\text{-}hm3Dq}$ mice [one-way analysis of variance (ANOVA) and Tukey post hoc test] (D; $n = 11$; saline:photostimulation, $P < 0.001$; saline:CNO-photostimulation, $P = 0.07$: photostimulation:CNO-photostimulation, $P < 0.001$), and LH$^{Vglut2\text{-}Fas\text{-}ChR2}$:DBB$^{Vglut2\text{-}hm3Dq}$ mice) (E; $n = 8$; saline:photostimulation, $P = 0.002$; saline:CNO-photostimulation, $P = 0.006$; photostimulation:CNO-photostimulation, $P = 0.88$). (**F**) Simultaneous recording of LH$^{Vgat\text{-}GCaMP6m}$ and DBB$^{Vgat\text{-}GCaMP6m}$ population activity during feeding bouts (shaded areas). (**G** and **H**) Effect of photostimulation of LH$^{Vgat\text{-}ChR2}$ cell bodies on DBB$^{Vgat\text{-}GCaMP6}$ neuronal activity at various frequencies (G) and pulse durations (H). $^{*}P < 0.05$; $^{**}P < 0.01$; $^{***}P < 0.001$.

fasted mice caused indiscriminate feeding when given access to both chow and HFD simultaneously (Fig. 4K). From these data, we concluded that DBB^{GABA} neurons respond to environmental cues of threat and reduce their activity during feeding. We also found that diazepam reduced DBB^{GABA} neuronal activity and recapitulated the indiscriminate feeding phenotype produced by LH^{GABA}→DBB^{GABA} activation.

DISCUSSION

In this study, we found a previously unidentified LH^{GABA}→DBB^{GABA} pathway that promotes feeding by suppressing environmentally driven anxiety. This projection likely acts in concert with other known projections of LH^{GABA} neurons to coordinate successful feeding (*20*–*24*). In vivo fiber photometry data show that DBB^{GABA} neurons respond to anxiogenic environmental stimuli and reduce activity during feeding. This is consistent with the known function of DBB neurons in promoting environment-responsive arousal (*8*–*10*). Our data thus suggest that LH^{GABA} neurons not only induce appetitive and consummatory behaviors but also alter sensitivity to the environment to promote feeding behavior. Since the induced feeding state observed here is indiscriminate, this suggests that some of the altered sensitivity may result via altered evaluation of food value itself. This aligns with the converse phenotype of picky eaters who have anxious personalities and with a study showing that activation of forebrain somatostatin neurons increases anxiety with selective consumption of a calorie-dense diet (*5*, *31*). We further explored this point and demonstrated that environmentally driven anxiety is a key mediator in the selection and proportion of low-value, but safe food consumed compared to high-calorie, but unsafe food. Moreover, the recapitulation of our circuit data with the effects with diazepam further points to the fundamental link between anxiety, food evaluation, and food consumption. Notably, despite verifying correct LH targeting, because of inherent variation associated with stereotaxic injections and the continuous distribution of GABAergic neurons between the LH and nearby regions, e.g., the dorsomedial hypothalamus, we could not completely rule out a

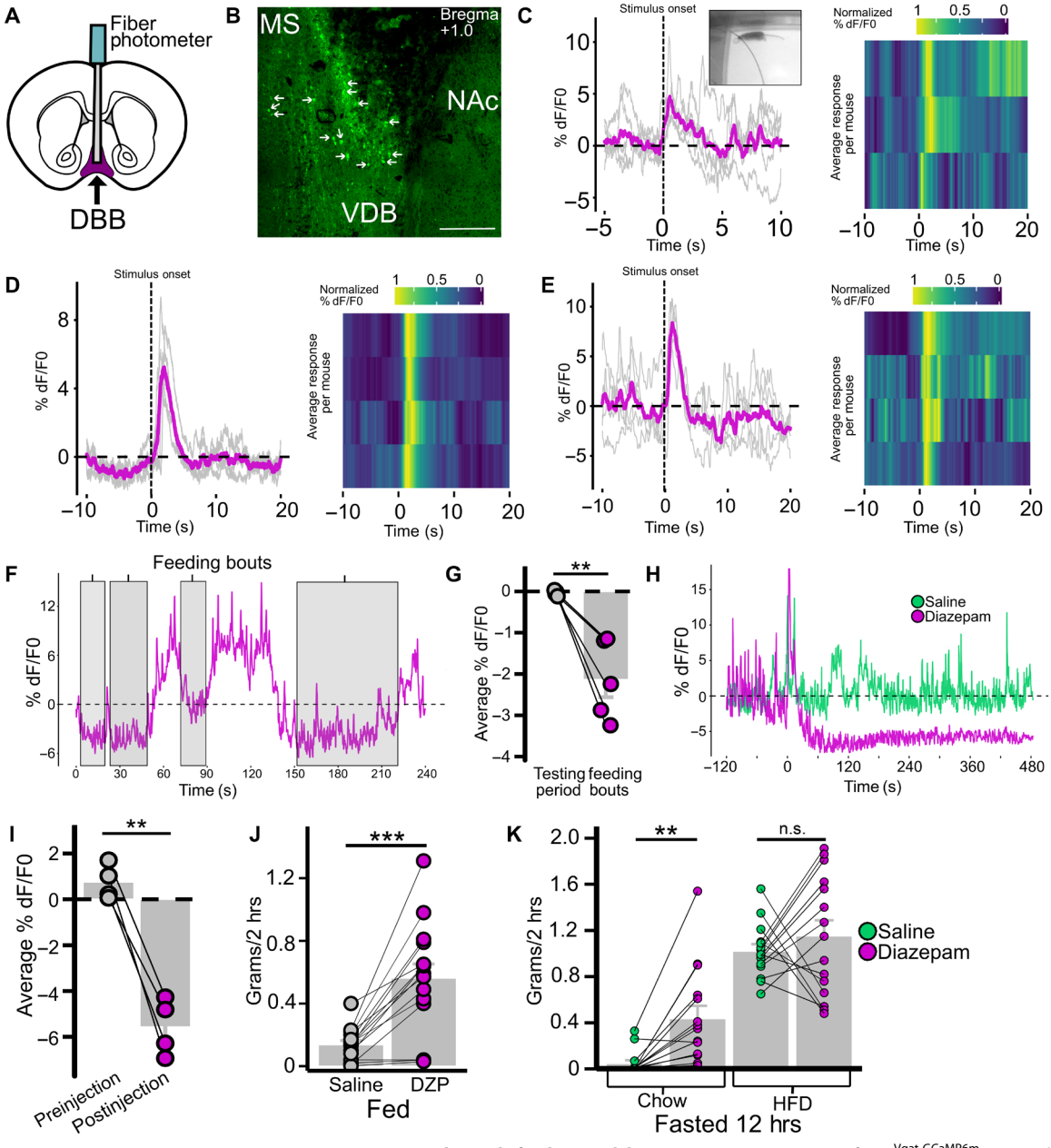

Fig. 4. DBB Vgat neurons are responsive to anxiogenic environmental stimuli, feeding, and diazepam. (**A** to **E**) Response of DBB$^{Vgat\text{-}GCaMP6m}$ neuronal population to threatening environmental stimuli. (A) Schematic of DBB$^{Vgat\text{-}GCaMP6m}$ injection and optic fiber placement strategy. (B) Brain slice with DBB$^{Vgat\text{-}GCaMp6m}$ neurons (VDB); arrows indicate cell bodies. MS, medial septum. (C to E) DBB$^{Vgat\text{-}GCaMP6m}$ neuronal activity change in response to stimulus (onset at 0 s) with gray traces indicating single interactions, magenta traces indicating averaged response, and heat map indicating normalized average responses per mouse in response to novel object interaction (C; inset shows stimulus onset), looming threat (D), and loud sound (E). (**F** and **G**) Response of DBB$^{Vgat\text{-}GCaMP6m}$ neurons to feeding in the fasted condition with representative trace during feeding bouts (F; shaded gray) and averaged activity during feeding bout compared to average activity over relevant testing period (G; $n = 5$, $P = 0.002$). (**H** to **K**) Effect of diazepam (DZP) on DBB$^{Vgat\text{-}GCaMp6}$ neuronal activity and feeding behavior. (H) Effect of intraperitoneal diazepam on DBB$^{Vgat\text{-}GCaMp6}$ neuronal activity in comparison with intraperitoneal saline; (I; $n = 4$, $P = 0.002$) Averaged activity 1.5 min before injection compared to average activity 3 to 4.5 min after injection. (J) Effect of intraperitoneal injection of saline versus diazepam on feeding ($n = 15$) when fed ($P < 0.001$). (K) Effect of diazepam on fasting-induced food intake of chow and HFD when presented with free access to both simultaneously for 2 hours (chow, $P = 0.001$; HFD, $P = 0.421$). *$P < 0.05$; **$P < 0.01$; ***$P < 0.001$.

slight contribution of nearby non-LH^{GABA} neurons in some mice tested in our study.

From a pharmacologic perspective, our data are notable because one of the most troubling aspects of nearly all psychotropic agents for anxiety and depression is their strong tendency to induce hunger, weight gain, and metabolic disease (*39*). These include drugs used for children with sensory processing disorders, such as risperidone for autism (*40*). Further, given recent compelling data demonstrating that LH^{GABA} neurons can be activated by the presence and consumption of rewarding foods and encode reward

prediction (*24*), it is conceivable that the LH^{GABA}→DBB^{GABA} neurocircuit may be involved in "stress eating," i.e., consumption of rewarding foods to reduce feelings of anxiety. A clinical example of this may be the compulsion to binge seen in binge-eating disorder after acute stress (*41*). Mechanistic demonstration of the direct link between the hedonic LH and the anxiogenic DBB provides tantalizing evidence that this heretofore difficult-to-define behavior in humans may have firm grounding in neurobiology. Knowledge of the neurocircuitry mediating the tight connection between hunger and anxiety provides a mechanistic platform for specific development of behavioral interventions and therapeutics against eating and anxiety-related disorders.

MATERIALS AND METHODS

Animal care

All mice were maintained in the Institute of Molecular Medicine semibarrier animal facility. They were housed at 21° to 22°C on a 12-hour light/dark cycle with standard pellet chow and water ad libitum—except in fasting experiments. Animal care and procedures were approved by the University of Texas Health Science Center at Houston Institutional Animal Care and Use Committee (IACUC). All IACUC guidelines were followed for care and use of mice. Strains of mice used in this study have been described previously: Pdx1-cre, Vgat-cre, Vglut2-cre (*22*, *23*, *28*). Male and female mice were used in roughly equal numbers as preliminary analysis revealed no significant difference in behavior. Multiple litters were used, and mice were at least 6 weeks old before surgery.

Neurosurgery

Stereotaxic surgery for the delivery of viral vectors to localized brain regions and for optical fiber implantation was performed as previously described, with 0.1-mm precision in the anterior-posterior (AP), mediolateral (ML), and dorsal-ventral (DV) axes (*22*). Mice were anesthetized with a ketamine/xylazine/acepromazine cocktail (80, 8, and 2.5 mg/kg); after confirmation of the absence of the pedal reflex, mice were affixed into the stereotaxic frame, and skin over the cranium was incised. Viral vectors were delivered with a 0.5-μl syringe (Neuros Model 7000.5 KH, point style 3; Hamilton, Reno, NV, USA) with the infusion rate controlled by a microinjector motor (Quintessential Stereotaxic Injector; Stoelting, Wood Dale, IL, USA) between 25 and 50 nl/min. Viral preparations were titered at ~1012 particles/ml. Coordinates for injection were as follows: AP −1.5, ML −0.9, and DV −5.1 (for LH); AP +1.1, ML −0.1, and DV −5 (for DBB). For optogenetic experiments, an uncleaved fiber optic cannula [Ø1.25-mm stainless ferrule, Ø200-μm core, 0.39 numerical aperture (NA); Thorlabs, Newton, NJ, USA] was cut to 4.8 to 5.0 mm in length for implant over the DBB. For fiber photometry, a precleaved wide-aperture fiber optic cannula (Ø1.25-mm stainless ferrule, Ø400-μm core, 0.66 NA; Doric Lenses, Quebec, QC, Canada) were implanted over the LH or DBB. For GABAzine and saline in vivo microinfusions, a guide cannula was placed over the DBB, which permitted preinjection of drug, before placing a removable optic fiber. Fast-drying acrylic glue and then dental cement were used to secure implantation before suture. Two injections of carprofen (5 mg/kg) were administered after surgical analgesia, 24 hours apart. All LH injections were unilateral since preliminary data showed no difference between right and left activation; DBB injections were centrally located (with 0.1-mm right shift to avoid sagittal sinus) and thus bilateral.

Viral vectors

The following plasmids that were packed in viral vectors were used for this study. Unless otherwise specified, each was packaged either in AAV serotype 2/9 or in DJ/8 by the Baylor College of Medicine Neuroconnectivity Core (B.R.A. and J.S.) or commercial sources.

AAV-Ef1α-FLEX-hChR2(H134R)-EYFP-WPRE-hGHpA (Addgene, 20298)

AAV-Ef1α-FLEX-hChR2(H134R)-EYFP-WPRE-pA (University of North Carolina Vector Core)

AAV-Ef1α-FLEX-EGFP-WPRE-pA (Baylor Neuroconnectivity Core)

AAV-Ef1α-FLEX-Syn::EGFP-WPRE-hGHpA (Baylor Neuroconnectivity Core)

AAV-Ef1α-FAS-ChR2(H134R)-mCherry-WPRE-pA (Addgene, 37090)

AAV-Ef1α-FLEX-TVA-mRuby (Baylor Neuroconnectivity Core)

AAV-EF1α-DIO-GCaMP6m-WPRE-pA (Baylor Neuroconnectivity Core)

AAV-Ef1α-DIO-hM3Dq-pA-mCherry (Baylor Neuroconnectivity Core)

(capsid AAV2/1) pAAV-Ef1a-EGFP-2A-iCre (Baylor Neuroconnectivity Core)

(capsid rAAV2-retro)AAV-Ef1a-iCre-P2A-H2B::Venus (Baylor Neuroconnectivity Core)

Brain slice electrophysiology

Coronal brain slices (250 to 300 μm) containing the DBB (centered around the ventral portion) were harvested from Cre+ mice at least 3 weeks after unilateral LH injection of AAV-FLEX-ChR2-EYFP or AAV-FAS-ChR2-mCherry. After inhalational anesthesia of isoflurane, mice were decapitated and brains were quickly harvested and preserved in ice-cold cutting solution. After slicing, the brains were incubated in 32°C artificial cerebrospinal fluid (aCSF) for an hour and then maintained at room temperature until used for recording. aCSF composition was as follows: 125 mM NaCl, 2.5 mM KCl, 1 mM $MgCl_2$, 2 mM $CaCl_2$, 1.25 mM NaH_2PO_4, 25 mM $NaHCO_3$, and 10 mM D-glucose, bubbled with 95% O_2/5% CO_2. During recording, slices were superfused with aCSF (2 ml/min) warmed at 32°C (feedback-controlled in-line heater TC-324B, Warner Instruments). Cells were identified through a 40× water-immersion objective with differential interference contrast and infrared illumination. DBB neurons were selected for recording if found medial to the islets of Cajal and below the horizontal midline and recording for the presence or absence of cre-dependent fluorescence in the pertinent experiments. Whole-cell voltage-clamp recordings were made using patch pipettes (3 to 5 megohms) filled with Cs^+-based low internal Cl^- solution, containing 135 mM $CsMeSO_3$, 10 mM Hepes, 1 mM EGTA, 3.3 mM QX-314, 4 mM Mg–adenosine triphosphate, 0.3 mM Na2–guanosine triphosphate, and 8 mM Na_2-phosphocreatine (pH 7.3 adjusted by CsOH; 295 mOsm). For ChR2-assisted circuit mapping, 473-nm laser light (Opto Engine LLC, Midvale, UT, USA) was pair-pulsed onto the DBB at 1 to 5 ms). When an inhibitory current (IPSC) was identified (no excitatory currents were identified), GABAzine (10 μM) was bath-perfused to block GABA-A receptors and eliminate the current. After recovery, tetrodotoxin (0.5 μM; Alomone Labs, Jerusalem, Israel) then 4-aminopyridine (100 μM;

Acros Organics, Fisher Scientific, Pittsburgh, PA, USA) was bath-applied to block action potentials and network activity, selecting only for photostimulation-induced monosynaptic currents.

Behavioral testing

All tests were conducted during the light cycle after at least 3 weeks of recovery from surgery in clean empty cages without bedding. For optogenetic feeding experiments, an integrated rotary joint patch cable connected the ferrule of the implanted optic fiber to the 473-nm diode-pumped solid-state laser (Opto Engine LLC, Midvale, UT, USA). Light pulse protocol (10 Hz with 50-ms pulses at ~10 to 15 mW/mm^2 was selected empirically on the basis of feeding data) was generated by a Master-8 pulse stimulator (A.M.P.I., Jerusalem, Israel). For the RTPP test, OFT, and competing choice feeding assays, the laser activity was routed through a Noldus EthoVision XT (Noldus Information Technology, Wageningen, Netherlands) behavioral chamber camera; EthoVision XT 11.5 software was used to control laser activity dependent on mouse position.

Feeding

Unless otherwise specified, mice were fed ad libitum in their home cages with standard pellet chow in their home cage before testing. All mice were previously exposed to HFD (Research Diets D12492; 20% protein, 60% fat, 20% carbohydrate, 5.21 kcal/g) in their home cage several days before tests with HFD. For Pdx1-cre mice, the amount of food consumed over a 15-min laser stimulation period was compared between Flex-ChR2–transfected and Flex-GFP–transfected mice. For Vgat-cre, amounts of food consumed per mouse over a 10-min prestimulation period, 10-min laser stimulation period, and 10-min post–laser stimulation period were compared. To determine food preference, mice were given free access to both regular chow and HFD during a 10-min laser stimulation period. To test competing preference for laser versus food, mice were habituated to the Noldus chamber for 10 min with laser paired to one side of the chamber and then, one of two paradigms was used: (i) regular chow was placed in laser on side, and HFD was placed in the laser off side; and (ii) regular chow was placed in the laser off side, and no food was placed in the laser on side. Latency to food consumption was calculated as the time spanning from the beginning of food exposure after a 24-hour fast or onset of laser stimulation and the first time the mouse bit the pellet.

Pharmacology

GABAzine or saline (~200 nl) was infused into the DBB via a guide cannula. The dose is comparable to other microinjection techniques targeting the basal forebrain in mice (*42*). After 15 min, an optic fiber connected to a cap was fixed into place into the guide cannula, and laser stimulation pulsed. For diazepam experiments, mice were intraperitoneally injected with either saline or diazepam (3 mg/kg) dissolved in 0.1% carboxymethyl cellulose at 1:10 dilution of stock dissolved in dimethyl sulfoxide (DMSO) and then placed into testing cage; timing began immediately after injection, with regular chow (ad libitum fed state) or regular chow and HFD (fasted state) placed into the testing cage with water. Food consumption was measured after 2 hours.

Clozapine-N-oxide

Two strains of mice were used: Vgat-cre with LHFlex-ChR2 and DBBDIO-GqDREADD, and Vglut2-cre with LHFas-ChR2 and DBBDIO-GqDREADD. Both had an optic fiber implanted over the DBB. These were injected with either saline or CNO (3 mg/kg at 1:15 stock solution in DMSO) and left in a testing chamber for 30 min. Food was measured, and then, mice were exposed to 10 min of laser stimulation; food was measured again afterward.

RTPP test, OFT, CPP test, and EPM

Pdx1-cre and Vgat-cre mice transfected with Flex-ChR2 or Flex-GFP were placed into the Noldus behavior chamber and had activity monitored for 20 min, with laser stimulation paired to one side of the chamber. Testing was initiated when mouse was in the laser off zone. Half of the mice in each group had the left side of the chamber paired with laser stimulation, and half with the right side, to counterbalance possible testing differences. Mouse movement was tracked and analyzed using EthoVision XT software (version 11.5; Noldus Information Technology, Wageningen, Netherlands). For the open field, the periphery of the chamber was determined as ~2 mouse (10 cm) widths; the patch remaining in the center is the "center." In the CPP test, this center area was paired with laser activation. For the EPM tests, mice fasted overnight were then placed on the center of the EPM and habituated for 10 min. Then, regular chow was placed on either the open or closed arm (see fig. S5 for HFD placed on the converse arm), and the mouse was then placed on the open arm with the food to allow discovery. Latency to food consumption was determined as above; the mice were allowed 10 min to consume food after first bite.

Fiber photometry

Equipment

All fiber photometry was conducted using a Doric Lenses setup, with a light-emitting diode (LED) driver controlling two connectorized LEDs (405 and 465 nm) routed through a five-port Fluorescence MiniCube [order code: FMC5_AE(405)_AF(420-450)_E1(460-490)_F1(500-550)_S] to deliver excitation light for calcium-independent and calcium-dependent signals to the implanted optic fiber simultaneously. Emitted light was received through the MiniCube and split into two bands—420 to 450 nm (autofluorescence: calcium-independent signal) and 500 to 550 nm (GCaMP6 signal: calcium-dependent signal). Each band was collected by a Newport 2151 Visible Femtowatt Photoreceiver module (photometer) with an add-on fiberoptic adaptor. Output analog signal was converted to digital signal through the fiber photometry console and recorded using the "Analog-In" function on Doric Studios (V4.1.5.2).

Behavioral tests

Looming threat. Mice are acutely sensitive to potential predatory presence and approach, and this stimulus is anxiogenic. Laboratory environments and the experimenter themselves induce a similar anxiogenic response, with close neurotheological correlates to predator response (1, 37, 38, 43). Thus, we used a meaningful predator stimulus for laboratory mice: the looming threat of an experimenter's hand. Mice were tested in their home cage with the roof removed; after 3 min of acclimation to the connected cable, the experimenter placed one hand 2 cage heights above the mouse for 3 s; and the onset of hand movement was set as time 0.

Loud sound. Similarly, mice are wary of loud sounds indicating potential danger. Mice were tested in their home cage with the roof removed; after 3 min of acclimation to the connected cable, the experimenter (positioned across the room out of sight of the mouse and immobile) clapped hands five times in rapid succession. The onset of clapping was set as time 0.

Novel object. Mice were placed in a testing chamber and acclimated for 10 min. Then, recording was initiated; 30 s after recording

onset, a novel object (15-ml Falcon tube cap) was placed in a corner of the cage. The novel object interaction onset was determined by the moment when the mouse's nose touched the novel object.

Fast-refeeding. After a 24-hour fast, mice were placed in a testing chamber and acclimated for 10 min. Then, recording was initiated; 30 s after recording onset, HFD and regular chow were placed into two different corners of the testing chamber. Food consumption bout onset was determined by the moment when the mouse bit the pellet (fecal consumption was excluded); food consumption bout offset was set when the mouse ceased chewing and began investigatory sniffing behaviors/rearing. Two experimenters (R.M.C. and M.J.) independently viewed the videos to determine the offset, and the averaged onset/offset time between the two was used.

Diazepam. Mice were habituated for 2 to 3 min with the cable attached in their home cage, and then, recording was started. After 2 min, mice were given an intraperitoneal injection of either saline or diazepam (3 mg/kg; Sigma-Aldrich) and were monitored for the next 20 min. No food or other stimulus was present during testing.

Data analysis

Data were acquired through Doric Studios V4.1.5.2. and saved as comma-separated files (header was deleted) at a sampling rate of either 1 or 2.5 kS/s. An in-house script (available upon request) written in R (V3.4.4. "Someone to Lean On," packages ggplot2, reshape, zoo, plyr, viridis, and scales) was used to calculate the baseline fluorescence (F0) using linear regression [compare (*36*)] across a chosen period of recording. The change in fluorescence (dF) was then determined from the residuals and multiplied by 100 to arrive at percentage of dF/F0. A sliding median with a window 51 data points in width was used to reduce noise. For looming threat, loud sound, and novel object, the baseline was calculated from 10 s before stimulus onset to 20 s after stimulus onset. For fast-refeeding, because mice typically engage in a series of quick successive feeding bouts, the F0 was calculated across a 50-s period with the feeding bout in the center. The average percentage of dF/F0 across the whole period was compared to the average percentage of dF/F0 during the feeding bout. For diazepam, 1.5 min before intraperitoneal injection was used to calculate the baseline, and this period was averaged and compared to a 1.5-min time segment occurring 5 min after intraperitoneal injection.

Stimulation frequency–dependent inhibition. For this test, there was leakage of laser-emitted light into the fiber photometer. Two filtering methods were applied: (i) a raw intensity cutoff slightly higher than the highest natural peak observed in the trace and (ii) a sliding median window 1800 sample points in width (~0.7 s) applied to eliminate remaining laser-induced artificial light increases.

Note: The calcium-independent fluorescence signal was also recorded during all tests. No significant alteration in signal level was observed compared to calcium-dependent signal (indicating steady LED excitation), so we do not display these data for simplicity except in movies S2 and S3.

Tissue section imaging and immunohistochemistry

To harvest brain tissue, mice were given a lethal injection of ketamine/xylazine/ acepromazine. After loss of the pedal reflex, mice were transcardially perfused with 15 ml of saline and 15 ml of 10% buffered formalin. The brain was then extracted and stored in 10% buffered formalin for at least 1 day, and then, the brain was switched to 30% sucrose solution and stored for at least 1 more day. Brains were frozen with dry ice on a microtome and sectioned into 30 μM slices. The slices were mounted onto microscope slides and coverslipped with Fluoromount (Diagnostic BioSystems Inc., Sigma-Aldrich). A confocal microscope was used to image the slices (Leica TCS SP5, Leica Microsystems, Wetzlar, Germany). For immunohistochemistry, brains were washed and placed in a blocking solution for 1 hour (10% donkey serum, 0.3% Triton X-100 dissolved in phosphate-buffered saline), and then incubated overnight at 4°C with the appropriate primary antibody. Then, after washing, they were incubated overnight at 4°C with the appropriate secondary antibody. Purple and green, rather than red and green, were used for ease of visual discrimination. The following antibodies were used:

Primary

c-Fos rabbit monoclonal antibody (mAb) (9F6) (#2250, Cell Signaling Technology)

Orexin A rabbit mAb (#H-003-30, Phoenix Pharmaceuticals)

Melanin-concentrating hormone rabbit mAb (#H-070-47, Phoenix Pharmaceuticals)

Secondary

Alexa Fluor 647–conjugated AffiniPure Donkey (H+L) anti-rabbit immunoglobulin G (Jackson ImmunoResearch)

Distance from bregma in millimeters is written next to the scale bar in each image; these are approximated with reference to Franklin and Paxinos (*44*).

Statistical analysis

Data were collected into organized Excel (2016) sheets and exported into tab-delimited format. All statistical tests were run using R (V3.4.4. "Someone to Lean On," packages ggplot2, reshape, zoo, plyr, viridis, and scales). Mice exposed to two different conditions were compared using two-tailed paired *t* test. When two different groups of mice are tested, they are compared using two-tailed Welch's unequal variance *t* test. For the CNO-blocked feeding test, a one-way ANOVA was used for the three conditions, and Tukey's honestly statistical difference test was used for post hoc analysis. Means and SE are displayed as gray bar graphs behind individual data points.

Fiber photometry heat map

Individual traces were aligned to zero at stimulus onset and averaged to produce an average trace. These averaged traces were then normalized from 0 to 1 using the R scales package; each mouse's scaled average trace was combined into a heat map. The viridis package was used to generate a colorblind-friendly color scheme for heat map.

SUPPLEMENTARY MATERIALS

Supplementary material for this article is available at http://advances.sciencemag.org/cgi/content/full/5/3/eaav1640/DC1

Fig. S1. Optogenetic targeting projections from LH neurons to neurons in the DBB.
Fig. S2. Electrophysiological recordings on DDB neurons that receive monosynaptic inputs from LH neurons.
Fig. S3. Tracing DDB neurons that receive direct inputs from LH.
Fig. S4. Tracing LH neurons that send direct projections to DBB neurons.
Fig. S5. LH^{GABA} neurons send direct projections to the DBB.
Fig. S6. Optogenetic stimulation of LH^{GABA} to DBB projections increased food-dependent exploratory behavior.
Fig. S7. Competition between anxiogenic conditions and feeding behavior.
Fig. S8. Verification of synthetic excitatory receptor (hm3Dq) expression in DBB neurons.
Movie S1. Activation of LH^{Vgat}→DBB fibers (laser ON) induces immediate increase in sniffing, licking, and exploratory behavior, followed by consumption of chow.
Movie S2. Fiber photometry data of novel object interaction.
Movie S3. Fiber photometry data of food consumption after 24-hour fasting.

REFERENCES AND NOTES

1. D. W. Grupe, J. B. Nitschke, Uncertainty and anticipation in anxiety: An integrated neurobiological and psychological perspective. *Nat. Rev. Neurosci.* **14**, 488–501 (2013).
2. D. Mobbs, J. J. Kim, Neuroethological studies of fear, anxiety, and risky decision-making in rodents and humans. *Curr. Opin. Behav. Sci.* **5**, 8–15 (2015).
3. J. L. Verdolin, Meta-analysis of foraging and predation risk trade-offs in terrestrial systems. *Behav. Ecol. Sociobiol.* **60**, 457–464 (2006).
4. S. A. Cermak, C. Curtin, L. G. Bandini, Food selectivity and sensory sensitivity in children with autism spectrum disorders. *J. Am. Diet. Assoc.* **110**, 238–246 (2010).
5. C. V. Farrow, H. Coulthard, Relationships between sensory sensitivity, anxiety and selective eating in children. *Appetite* **58**, 842–846 (2012).
6. A. M. Smith, S. Roux, N. T. Naidoo, D. J. L. Venter, Food choices of tactile defensive children. *Nutrition* **21**, 14–19 (2005).
7. W. H. Kaye, C. M. Bulik, L. Thornton, N. Barbarich, K. Masters; Price Foundation Collaborative Group, Comorbidity of anxiety disorders with anorexia and bulimia nervosa. *Am. J. Psychiatry* **161**, 2215–2221 (2004).
8. Å. K. Johansson, Å. H. Bergvall, S. Hansen, Behavioral disinhibition following basal forebrain excitotoxin lesions: Alcohol consumption, defensive aggression, impulsivity and serotonin levels. *Behav. Brain Res.* **102**, 17–29 (1999).
9. C. Anaclet, N. P. Pedersen, L. L. Ferrari, A. Venner, C. E. Bass, E. Arrigoni, P. M. Fuller, Basal forebrain control of wakefulness and cortical rhythms. *Nat. Commun.* **6**, 8744 (2015).
10. M. Goard, Y. Dan, Basal forebrain activation enhances cortical coding of natural scenes. *Nat. Neurosci.* **12**, 1444–1449 (2009).
11. K. Kai, M. Hashimoto, K. Amano, H. Tanaka, R. Fukuhara, M. Ikeda, Relationship between eating disturbance and dementia severity in patients with Alzheimer's disease. *PLOS ONE* **10**, e0133666 (2015).
12. M. Ikeda, J. Brown, A. Holland, R. Fukuhara, J. Hodges, Changes in appetite, food preference, and eating habits in frontotemporal dementia and Alzheimer's disease. *J. Neurol. Neurosurg. Psychiatry* **73**, 371–376 (2002).
13. A. M. Herman, J. Ortiz-Guzman, M. Kochukov, I. Herman, K. B. Quast, J. M. Patel, B. Tepe, J. C. Carlson, K. Ung, J. Selever, Q. Tong, B. R. Arenkiel, A cholinergic basal forebrain feeding circuit modulates appetite suppression. *Nature* **538**, 253–256 (2016).
14. J. N. Betley, S. Xu, Z. F. H. Cao, R. Gong, C. J. Magnus, Y. Yu, S. M. Sternson, Neurons for hunger and thirst transmit a negative-valence teaching signal. *Nature* **521**, 180–185 (2015).
15. Y. Chen, Y.-C. Lin, C. A. Zimmerman, R. A. Essner, Z. A. Knight, Hunger neurons drive feeding through a sustained, positive reinforcement signal. *eLife* **5**, e18640 (2016).
16. C. J. Burnett, C. Li, E. Webber, E. Tsaousidou, S. Y. Xue, J. C. Brüning, M. J. Krashes, Hunger-driven motivational state competition. *Neuron* **92**, 187–201 (2016).
17. M. O. Dietrich, M. R. Zimmer, J. Bober, T. L. Horvath, Hypothalamic Agrp neurons drive stereotypic behaviors beyond feeding. *Cell* **160**, 1222–1232 (2015).
18. S. L. Padilla, J. Qiu, M. E. Soden, E. Sanz, C. C. Nestor, F. D. Barker, A. Quintana, L. S. Zweifel, O. K. Rønnekleiv, M. J. Kelly, R. D. Palmiter, Agouti-related peptide neural circuits mediate adaptive behaviors in the starved state. *Nat. Neurosci.* **19**, 734–741 (2016).
19. J. H. Jennings, R. L. Ung, S. L. Resendez, A. M. Stamatakis, J. G. Taylor, J. Huang, K. Veleta, P. A. Kantak, M. Aita, K. Shilling-Scrivo, C. Ramakrishnan, K. Deisseroth, S. Otte, G. D. Stuber, Visualizing hypothalamic network dynamics for appetitive and consummatory behaviors. *Cell* **160**, 516–527 (2015).
20. E. H. Nieh, G. A. Matthews, S. A. Allsop, K. N. Presbrey, C. A. Leppla, R. Wichmann, R. Neve, C. P. Wildes, K. M. Tye, Decoding neural circuits that control compulsive sucrose seeking. *Cell* **160**, 528–541 (2015).
21. Y. Li, J. Zeng, J. Zhang, C. Yue, W. Zhong, Z. Liu, Q. Feng, M. Luo, Hypothalamic circuits for predation and evasion. *Neuron* **97**, 911–924.e5 (2018).
22. L. R. Mangieri, Y. Lu, Y. Xu, R. M. Cassidy, Y. Xu, B. R. Arenkiel, Q. Tong, A neural basis for antagonistic control of feeding and compulsive behaviors. *Nat. Commun.* **9**, 52 (2018).
23. Z. Wu, E. R. Kim, H. Sun, Y. Xu, L. R. Mangieri, D.-P. Li, H.-L. Pan, Y. Xu, B. R. Arenkiel, Q. Tong, GABAergic projections from lateral hypothalamus to paraventricular hypothalamic nucleus promote feeding. *J. Neurosci.* **35**, 3312–3318 (2015).
24. M. J. Sharpe, N. J. Marchant, L. R. Whitaker, C. T. Richie, Y. J. Zhang, E. J. Campbell, P. P. Koivula, J. C. Necarsulmer, C. Mejias-Aponte, M. Morales, J. Pickel, J. C. Smith, Y. Niv, Y. Shaham, B. K. Harvey, G. Schoenbaum, Lateral hypothalamic GABAergic neurons encode reward predictions that are relayed to the ventral tegmental area to regulate learning. *Curr. Biol.* **27**, 2089–2100.e5 (2017).
25. B. Zingg, X.-l. Chou, Z.-g. Zhang, L. Mesik, F. Liang, H. W. Tao, L. I. Zhang, AAV-mediated anterograde transsynaptic tagging: Mapping corticocollicular input-defined neural pathways for defense behaviors. *Neuron* **93**, 33–47 (2017).
26. D. G. R. Tervo, B.-Y. Hwang, S. Viswanathan, T. Gaj, M. Lavzin, K. D. Ritola, S. Lindo, S. Michael, E. Kuleshova, D. Ojala, C.-C. Huang, C. R. Gerfen, J. Schiller, J. T. Dudman, A. W. Hantman, L. L. Looger, D. V. Schaffer, A. Y. Karpova, A designer AAV variant permits efficient retrograde access to projection neurons. *Neuron* **92**, 372–382 (2016).
27. I. Villano, A. Messina, A. Valenzano, F. Moscatelli, T. Esposito, V. Monda, M. Esposito, F. Precenzano, M. Carotenuto, A. Viggiano, S. Chieffi, G. Cibelli, M. Monda, G. Messina, Basal forebrain cholinergic system and orexin neurons: Effects on attention. *Front. Behav. Neurosci.* **11**, 10 (2017).
28. L. Vong, C. Ye, Z. Yang, B. Choi, S. Chua Jr., B. B. Lowell, Leptin action on GABAergic neurons prevents obesity and reduces inhibitory tone to POMC neurons. *Neuron* **71**, 142–154 (2011).
29. M. Schneeberger, K. Tan, A. R. Nectow, L. Parolari, C. Caglar, E. Azevedo, Z. Li, A. Domingos, J. M. Friedman, Functional analysis reveals differential effects of glutamate and MCH neuropeptide in MCH neurons. *Mol. Metab.* **13**, 83–89 (2018).
30. C. Blanco-Centurion, E. Bendell, B. Zou, Y. Sun, P. J. Shiromani, M. Liu, VGAT and VGLUT2 expression in MCH and orexin neurons in double transgenic reporter mice. *IBRO Rep.* **4**, 44–49 (2018).
31. C. Zhu, Y. Yao, Y. Xiong, M. Cheng, J. Chen, R. Zhao, F. Liao, R. Shi, S. Song, Somatostatin neurons in the basal forebrain promote high-calorie food intake. *Cell Rep.* **20**, 112–123 (2017).
32. S. R. Bodnoff, B. Suranyi-Cadotte, R. Quirion, M. J. Meaney, A comparison of the effects of diazepam versus several typical and atypical anti-depressant drugs in an animal model of anxiety. *Psychopharmacology* **97**, 277–279 (1989).
33. I. Gritti, P. Henny, F. Galloni, L. Mainville, M. Mariotti, B. E. Jones, Stereological estimates of the basal forebrain cell population in the rat, including neurons containing choline acetyltransferase, glutamic acid decarboxylase or phosphate-activated glutaminase and colocalizing vesicular glutamate transporters. *Neuroscience* **143**, 1051–1064 (2006).
34. A. Saunders, A. J. Granger, B. L. Sabatini, Corelease of acetylcholine and GABA from cholinergic forebrain neurons. *eLife* **4**, e06412 (2015).
35. A. Saunders, C. A. Johnson, B. L. Sabatini, Novel recombinant adeno-associated viruses for Cre activated and inactivated transgene expression in neurons. *Front. Neural Circuits* **6**, 47 (2012).
36. T.-W. Chen, T. J. Wardill, Y. Sun, S. R. Pulver, S. L. Renninger, A. Baohan, E. R. Schreiter, R. A. Kerr, M. B. Orger, V. Jayaraman, L. L. Looger, K. Svoboda, D. S. Kim, Ultrasensitive fluorescent proteins for imaging neuronal activity. *Nature* **499**, 295–300 (2013).
37. E. J. Chesler, S. G. Wilson, W. R. Lariviere, S. L. Rodriguez-Zas, J. S. Mogil, Influences of laboratory environment on behavior. *Nat. Neurosci.* **5**, 1101–1102 (2002).
38. J. C. Crabbe, D. Wahlsten, B. C. Dudek, Genetics of mouse behavior: Interactions with laboratory environment. *Science* **284**, 1670–1672 (1999).
39. J. P. Domecq, G. Prutsky, A. Leppin, M. B. Sonbol, O. Altayar, C. Undavalli, Z. Wang, T. Elraiyah, J. P. Brito, K. F. Mauck, M. H. Lababidi, L. J. Prokop, N. Asi, J. Wei, S. Fidahussein, V. M. Montori, M. H. Murad, Drugs commonly associated with weight change: A systematic review and meta-analysis. *J. Clin. Endocrinol. Metab.* **100**, 363–370 (2015).
40. C. J. McDougle, L. Scahill, M. G. Aman, J. T. McCracken, E. Tierney, M. Davies, L. E. Arnold, D. J. Posey, A. Martin, J. K. Ghuman, B. Shah, S. Z. Chuang, N. B. Swiezy, N. M. Gonzalez, J. Hollway, K. Koenig, J. J. McGough, L. Ritz, B. Vitiello, Risperidone for the core symptom domains of autism: Results from the study by the Autism Network of the Research Units on Pediatric Psychopharmacology. *Am. J. Psychiatry* **162**, 1142–1148 (2005).
41. K. R. Naish, M. Laliberte, J. MacKillop, I. M. Balodis, Systematic review of the effects of acute stress in binge eating disorder. *Eur. J. Neurosci.*, 1–15 (2018).
42. R. Sharma, P. Sahota, M. M. Thakkar, Nicotine administration in the cholinergic basal forebrain increases alcohol consumption in C57BL/6J mice. *Alcohol. Clin. Exp. Res.* **38**, 1315–1320 (2014).
43. C. Belzung, W. El Hage, N. Moindrot, G. Griebel, Behavioral and neurochemical changes following predatory stress in mice. *Neuropharmacology* **41**, 400–408 (2001).
44. K. B. J. Franklin, G. Paxinos, *The Mouse Brain in Stereotaxic Coordinates, Compact: The Coronal Plates and Diagrams* (Academic Press, ed. 3, 2008).

Acknowledgments: We would like to thank E. Walters for stimulating discussion that aided our conceptualization of this project and Z. Mao for help with microscopy. Q.T. is the guarantor of this work and, as such, had full access to all the data in the study and takes responsibility for the integrity of the data and the accuracy of the data analysis. **Funding:** This study was supported by NIH R01 DK114279 to Q.T., NIH 5F31DA041703 to L.R.M., NIH R01DK117281 and R01DK101379 to Yong Xu, and R01DK109934 to B.R.A. and Q.T. We also acknowledge the Neuroconnectivity Core funded by NIH IDDRC grant 1 U54 HD083092 for providing AAV vectors. Q.T. is the holder of the Cullen Chair in Molecular Medicine at

McGovern Medical School. R.M.C. was supported by the TL1 training grant 4TL1TR000369 (Center for Clinical and Translational Sciences, UTHealth). M.J. was supported by GradSURP (UTHealth). **Author contributions:** Conceptualization and writing: Q.T. and R.M.C.; investigation: R.M.C., Y.L., M.J., B.F.-O., J.B.-T., Yuanzhong Xu, and L.R.M.; resources: J.S., Yong Xu, and B.R.A.; supervision: Q.T.; and funding acquisition: Q.T. and B.R.A. **Competing interests:** The authors declare that they have no competing interests. **Data and materials availability:** All data needed to evaluate the conclusions in the paper are present in the paper and/or the Supplementary Materials. Additional data related to this paper may be requested from the authors.

Submitted 20 August 2018
Accepted 28 January 2019
Published 6 March 2019
10.1126/sciadv.aav1640

Citation: R. M. Cassidy, Y. Lu, M. Jere, J.-B. Tian, Y. Xu, L. R. Mangieri, B. Felix-Okoroji, J. Selever, Y. Xu, B. R. Arenkiel, Q. Tong, A lateral hypothalamus to basal forebrain neurocircuit promotes feeding by suppressing responses to anxiogenic environmental cues. *Sci. Adv.* **5**, eaav1640 (2019).